Comparative Analysis of Different Current Turbine Designs Based on Relevant Conditions of the Nile River of Egypt

Alsayed M. Hamouda 1*, Abdelrahman S. Abutaleb 1, Shady S. Rofail 1, Ahmed S. Shehata 1, A.H. Elbatran 1

1: Arab Academy for Science, Technology and Maritime Transport, Alexandria, P.O. Box 1029, Egypt
1* E-mail: alsayed050@gmail.com
1* Telephone: +201555591334

1. Abstract

Egypt is regarded as a developing country looking for increasing its renewable energy share to meet its sustainable development goal through utilizing as many renewable energy resources as possible and develop new technologies to harvest this energy at a maximum efficiency. One of these resources is water current present of the Nile. Hydrokinetic turbines can be used to harvest the kinetic energy. Vertical Axis hydrokinetic (Water) turbines (VAWTs) are gaining popularity nowadays in the market of hydrogenated renewable energy. The purpose of the present work is to investigate the performance of two different hydrokinetic turbines types: Savonius; and Darrius relative to local conditions of Egypt by conducting a 2D simulation for Darrieus and Savonius turbines Using ANSYS fluent 19.1. The study yields a 47% increase in Coefficient of power of Darrius turbine relative to that of the Savonieus turbine.

2. Keywords

Current Energy; Nile River; Savonius Turbine; Darrieus Turbine; CFD simulation

3. Introduction

3.1 General

The global energy demand continues to increase with the majority of this demand coming from developing countries. Such ongoing increase is mainly met by consumption of fossil fuels -which are already accounting for the majority of global energy consumption- resulting in an environmental degradation due to the accompanied emissions [1]. Also being finite energy sources promotes renewable energy sources to be the major energy supplier worldwide in the near future due to being environmentally friendly and guaranteeing sustainability. As a result, all sectors has been urged to adopt renewable energy sources and cut down emissions with the maritime sector being no exception. The maritime sector answer to this was adopting new approaches to cut down emissions and exploitation opportunities for offshore wind, water tides and water currents.

Since Egypt is regarded as a developing country [2], so developing reliable, efficient energy production techniques for potential renewable sources shall cut down the country fossil fuels dependence by a considerable margin in the years to come. One of the most promising renewable sources within the country is the water current in the vast network of 40,000 km of channels branching from the Nile River through hierarchically classified canals: principal (water directly from the Nile), main branches and distributary canals [3]. In addition, there are also mesqas, private ditches distributing water to the field. The

preceding implies that Current energy from flowing water in open channels has the potential to support local electricity needs with lower regulatory or capital investment than impounding water with more conventional means.

The theory of current stream power is similar to wind power but advantageous in being more predictable in velocities and direction of the fluid and hence more predictable power generation, adds to this water density is more than 800 times that of air, hence smaller scale hydrokinetic turbines are needed to extract the same power at even lower velocities if compared to wind turbines.

Hydrokinetic turbines are a flowing water energy converters which can be classified into horizontal axis water (hydrokinetic) turbines (HAWTs) and vertical axis water turbines (VAWTs). Both turbines have advantages and disadvantages. In comparison to the high power Coefficients of HAWTs, VAWTs can harvest energy from the flowing water from any direction [4] which means that a yaw mechanism is not necessary [5]. Vertical axis water turbines can be mainly categorized into lift-based Darrieus turbines and drag-based Savonius turbines [6].

3.2 Darrieus Turbine

Darrieus have been receiving much attention in recent years for being able to be used in stand-alone applications [7]. Ease of maintenance, simple blade fabrication, and low noise level, and its high efficiency in turbulent flow fields are just some advantages of Darrieus water turbines [8]. A great deal of research was carried out in the recent years by researchers to study the performance of Darrieus turbines. A study made by Mohamed [9] on the performance of Darrieus turbine with different shapes of airfoils investigated that the S-1046 shows a maximum power Coefficient of 0.4. An experimental investigation on the effect of different parameters on the performance of Darrieus turbine such as water flow velocity, and number of blades are carried out by shiono [10] which concluded that two bladed turbine is more efficient than three bladed turbine. A study carried out by Mahdi [11] on the startup characteristics of the H-Darrieus turbine concluded that the combined use of cambered airfoil NACA-2418 and the outward pitch angle of 1.5 degree resulted in a reduction of 27% of the starting time.

3.3 Savonius turbine

Savonius turbine is characterized by its low efficiency and high self-starting capabilities if compared to Darrieus turbine. A great deal of research has been carried out in recent years to improve the performance of Savonius turbine. A study made by Mohamed [12] proved that two bladed rotor have better performance than three bladed rotor. Regarding the effect of blade profile, Nur [13] studied the effect of Semicircular and elliptic shapes concluding that semicircular showed a better performance that elliptic shape. Khan [14] studied the performance of one stage, two stage, and three stage Savonius rotor to determine the most suitable rotor for micro sea floor power system concluding that two stage rotor gives a maximum power Coefficient of 0.049.

3.4 Objective of the study

Due to the lack of research on the Darrieus and Savonius turbines under the Conditions relative to Nile River, a study needs to be

performed to investigate the performance of both turbines to attain the optimum tip speed ratio, maximum power coefficient, starting torque and the behavior of power coefficient of the range of water speeds in Nile River. This was achieved by 2D simulation of both turbines using ANSYS software.

4. Principles of operation

The basic shape of a Darrieus turbine is an 'H' shape type, having two, three or four airfoils attached the central shaft with struts. According to the standard airfoil theory, if an airfoil is positioned with an angle of attack (α) in a fluid flow, a lift force (F_L) will be generated perpendicular to the direction of the free stream with a drag force (F_D) in the direction of the free stream as Shown in Fig. (1). The resultant of the lift and drag force can be resolved into an axial force normal to airfoil cord and a tangential force in the direction of rotation which is responsible for the torque and power output of the turbine. So Darrieus Turbine is a lift dependent turbine [9].

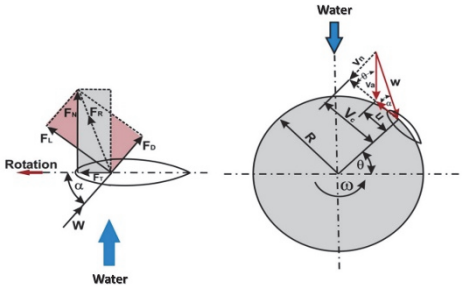

Fig. (1): Darrieus turbine illustration and Force analysis

On the other hand, a Savonius turbine is mainly a drag dependent turbine. The basic shape of a Savonius turbine is an 'S' shape type, having two semicircular blades attached to the central shaft. The operation principle of a Savonius turbine mainly depends on the difference of the drag force between the concave and convex blades of the turbine as Shown in Fig. (2). the drag coefficient of the concave side is much higher than the convex side. This difference

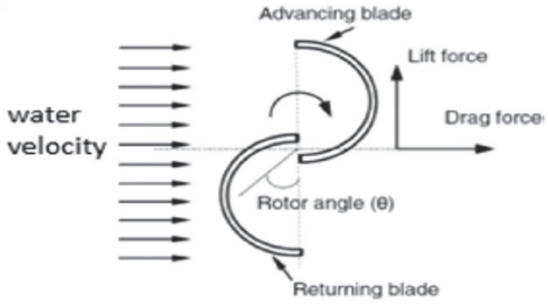

Fig. (2): Savonius turbine illustration and force analysis

create a moment around the central shaft of the turbine to which the blades are attached. This moment is responsible for the torque and power output of the turbine [15].

For a Darrieus and Savonius turbine of height H and Incoming Flow velocity V, the maximum power output can be written as follows $P = \frac{1}{2}\,\rho\,A\,V^3$ **(Eq.1)**

According to Betz's limit [16], a fraction of the kinetic energy crossing the turbine can be captured, this fraction can be expressed by power Coefficient (Cp).

$$C_P = \lambda\, C_T \qquad \textbf{(Eq.2)}$$

Where C_T is the Coefficient of torque and λ is the tip speed ratio.

$$C_T = \frac{T}{\frac{1}{2}\rho A R V^3} \qquad \textbf{(Eq.3)}$$

$$\lambda = \frac{\omega r}{V} \qquad \textbf{(Eq.4)}$$

5. Governing equations

Three assumptions were used during modelling which are:

1- Flow is incompressible.
2- Flow exhibits turbulent unsteady behavior.
3- Forced rotation of the rotor since the sliding mesh technique has been used. [17].

ANSYS Fluent 19.1 has been used to solve the Unsteady Reynolds averaged Navier-Stocks Equations (URANS) Formulated by

the Eq.5 and Eq.6 coupled with the $k-\varepsilon$ turbulence model expressed by Eq.7 and Eq.8.

1 - *Continuity and conservation of mass:*

Mass conservation principle presented by the continuity equation is expressed Eq.5 [18].

$$\frac{\partial \rho}{\partial t} + \nabla \cdot \rho \, u = 0$$

(Eq.5)

2 - *Momentum balance Equation:*

The momentum balance equation can be expressed by Eq.6.

$$\frac{\partial \rho u}{\partial t} + \nabla \cdot (\rho \, uu) = -\nabla P + \nabla \tau + \rho f$$

(Eq.6)

3 - *Transport equation for turbulent kinetic energy K* [19]

$$\frac{\partial \rho k}{\partial t} + \frac{\partial \rho k u_i}{\partial x_i} = \frac{\partial \left(\Gamma_k \frac{\partial k}{\partial x_j} \right)}{\partial x_j} + \tilde{G}_k - Y_k + S_k \quad \textbf{(Eq.7)}$$

4 - *Transport equation for dissipation of the specific energy ω* [20]

$$\frac{\partial \rho \omega}{\partial t} + \frac{\partial \rho \omega u_i}{\partial x_i} = \frac{\partial \left(\Gamma_\omega \frac{\partial \omega}{\partial x_j} \right)}{\partial x_j} + \tilde{G}_\omega - Y_\omega + D_\omega + S_\omega \quad \textbf{(Eq.8)}$$

6. CFD Model Setup

6.1 Model Geometry

Many researches on Darrieus turbines has employed different airfoil series; NACA 0012 was studied and shows a better operation in specific ranges of Reynolds numbers, after that focus goes to NACA0015, NACA0018, and NACA0022.Also a research on the Symmetric and non-symmetric blades based on five different series of the profile (NACA 00XX, NACA 63XXX, S-series, A-series and FX-series) have been made by M.H.Mohamed [9] concluded that S-1046 shows the maximum power coefficient among the considered series. In the present study, the S-1046 airfoil with a cord length (c) of 150 mm have been used as a purpose of validation.

Based on a review made by Kumar. [15] On Savonius turbine on the different parameters affecting turbine performance and a study made by Nur. [13] On Different blade profiles. In the present study, a two bladed Savonius turbine of semicircular profile with a Zero overlap ratio has been used for the purpose of validation.

In this study, the computational domain for Darrieus turbine was divided into five regions: a circular rotating Hub, a rectangular stationary far field and three rotating Control Circuits (CC) around the blades as shown below in Fig. (3). For Savonius turbine the domain -as in Fig. (4)- Is divided into two regions: a circular rotating hub, and a rectangular stationary far field.

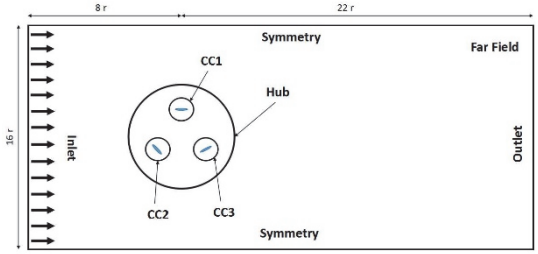

Fig. (3): Darrieus turbine Computational Domain.

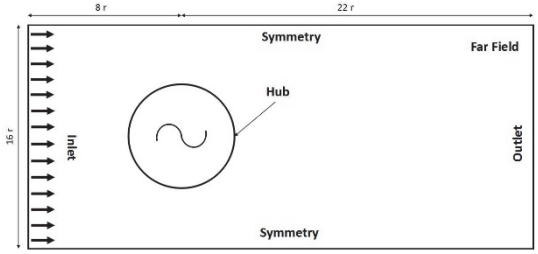

Fig. (4): Savonius turbine Computational Domain.

In order to avoid any blockage effect and reach a fully developed state of the turbine a research is conducted to find the optimum dimensions of the computational domain. Based on the well-referenced sensitivity analysis made by Mahdi [11]. A domain with a dimensions of 30 r and 16 r in the directions parallel and perpendicular to the

flow direction respectively. The turbine was located at 8 r from the inlet. Tables (1) and (2) below give a detailed description of the turbine design prepared by AutoCAD for Darrieus and Savonius Respectively.

Parameter	Value
Diameter [mm]	1000
Air foil	S – 1046
Cord length [mm]	150
Number of blades	3
Solidity	0.45
TSR range	1 – 3.5

Table 1: Darrieus turbine Specifications

Parameter	Value
Diameter [mm]	300
Blade profile	Semicircle
Overlap	zero
Number of blades	2
TSR range	0.4 – 1.2

Table 2: Savonius turbine Specifications

6.2 Meshing Topology

The quality and the method of the grid has a great effect on model accuracy and validity. Some techniques were used during the grid generation process to assure the accuracy and quality of the mesh. Unstructured grid is used, giving flexibility for an Automatic generation of grid. Attention paid to the modeling the boundary layer near walls which enhances the turbulence allowing it to reach its calibrated performance and give a better prediction of the fluid flow behavior near walls [21]. The quality of the mesh on the turbine blades is governed by the dimensionless y+ which is equal to 1 in the present study as suggested by other studies [24].The grid used has 15 layers of quadrilateral cells near airfoil wall, with the first cell height of about 5 x 10^{-2} mm (= 0.033% c) and 16 x 10^{-2} for Darrieus and Savonius respectively with a growth rate of 1.1. Adaption has been applied for the cells near the wall as Shown in Fig (5)

For increasing the mesh refinement and hence the results. A combination of Body sizing for hub, control circuits and far field, edge sizing for blades and interfaces has been used as seen in table (3) and (4) for Darrieus and Savonius Respectively.

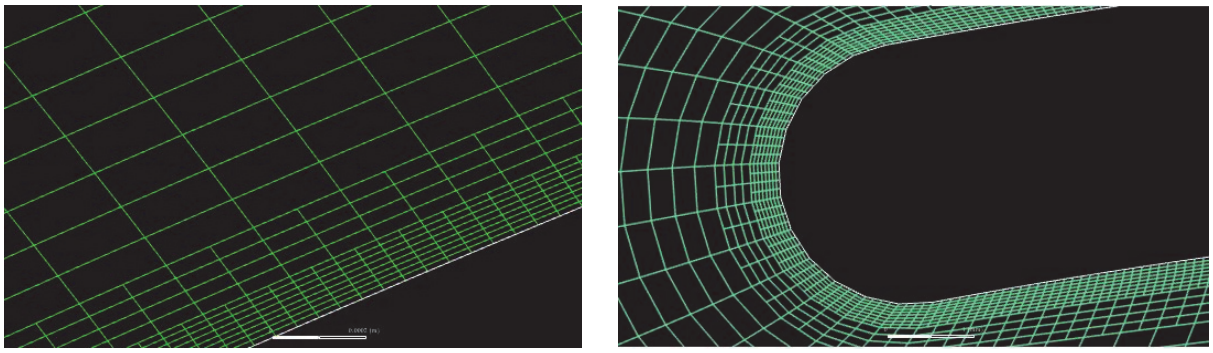

Fig. (5): Adaption for Darrieus turbine airfoil –left- & Savonius turbine blade –Right.

Item	Refinement levels			
	Level 1	Level 2	Level 3	Level 4
Far Field [mm]	50	47	44	41
Hub sizing [mm]	10	9	8	7
CC sizing [mm]	8	7	6	5
Edge sizing for CC	500	700	900	1100
Edge sizing for Hub	1000	1200	1400	1600
Edge sizing for blades [mm]	1	0.8	0.6	0.4
Number of cells	289391	358725	393901	572556

Table 3: Mesh Specification for Darrius turbine

Item	Refinement levels			
	Level 1	Level 2	Level 3	Level 4
Far Field [mm]	50	47	44	41
Hub sizing [mm]	5	4	3	2
Edge sizing for Hub	800	1000	1200	1400
Edge sizing for blades [mm]	0.6	0.5	0.4	0.3
Number of cells	220212	260350	313237	463405

Table 4: Mesh Specifications for Savonius turbine

6.3 Boundary Condition

For the present study, a velocity inlet was placed at the left of the computational domain with a uniform velocity profile of 2 m/s for the steady simulations. A pressure outlet was applied for the outlet at the right of the domain with a zero relative pressure representing an open condition. Further, the turbulent Intensity and turbulent viscosity ratio are 5% and 10 respectively and they are kept constant. For sides, a symmetry boundary condition is applied to avoid any side blockage effect. A no-slip wall boundary condition is assigned for the blades. Since there were no reported data regarding the effect of surface roughness in the validation set, it is neglected in the present study and will be studied in further research.

As shown in Fig. (6) For Darrieus turbine, Four interfaces – to insure continuity in the flow – have been created; three of them between the control circuits and the Hub and a large interface between the Hub and the Fairfield. For Savonius turbine, only one interface is created between the Hub and the far field as shown in Fig. (7).

For the transient simulation, Sliding mesh technique has been used for the rotating Hub at constant speed. The three control circuits and the blades were set to be rotating relative to the hub at constant velocity.

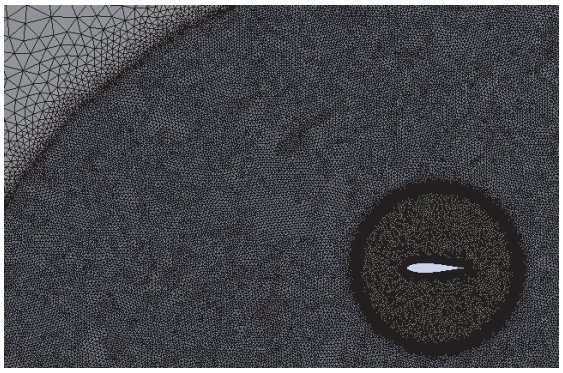

Fig. (6): Darrius turbine grid interfaces –portion.

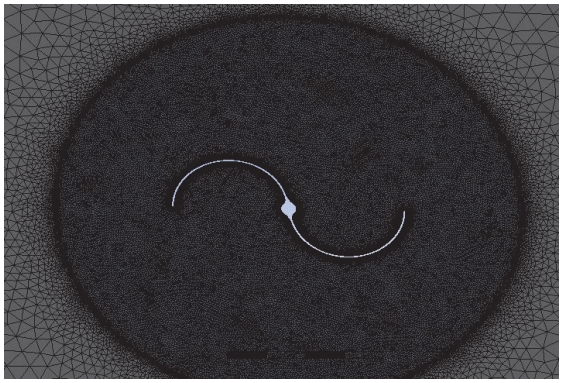

Fig. (7): Savonius turbine grid interfaces.

6.4 Turbulence Modeling

The turbulence model is a key parameter in any CFD Simulations as affects the resultant flow field and the computational resources as well. For complex simulation such as VAWTs, it is essential to choose appropriately the turbulence model especially for operation at low TSR values. Therefore, a particular attention was paid to the turbulence modeling.

In present study, the two equation realizable $k-\varepsilon$ turbulence model with a scalable wall function – for wall treatment – was used as recommended by earlier studies [9] [22]. The realizable $k-\varepsilon$ turbulence model is different form the

standard $k-\varepsilon$ turbulence model as it provides better performance in flows involving flow separation, recirculation, and rotation with a slight increase in computational resources [22]. The term ' realizable 'means the model is consistent with turbulent flows and satisfies certain mathematical constraints on Reynolds stresses [21].

The transport equations for k and ε in the realizable $k-\varepsilon$ turbulence model are given by the following equations [23].

$$\frac{\partial}{\partial t}(\rho k)+\frac{\partial}{\partial x_j}(\rho k u_j)=\frac{\partial}{\partial x_j}\left[\left(\mu+\frac{\mu_t}{\sigma_k}\right)\frac{\partial k}{\partial x_j}\right]+G_k+G_b-\rho\varepsilon-Y_M+S_k \quad \textbf{(Eq.9)}$$

$$\frac{\partial}{\partial t}(\rho \varepsilon)+\frac{\partial}{\partial x_j}(\rho \varepsilon u_j)=\frac{\partial}{\partial x_j}\left[\left(\mu+\frac{\mu_t}{\sigma_k}\right)\frac{\partial \varepsilon}{\partial x_j}\right]+\rho C_1 S_\varepsilon-\rho C_2\frac{\varepsilon^2}{k+\sqrt{\nu\varepsilon}}-C_{1\varepsilon}\frac{\varepsilon}{k}C_{3\varepsilon}G_b+S_\varepsilon \quad \textbf{(Eq.10)}$$

6.5 Mesh Independence study

In this study, a grid independence study was made for the purpose of verification that the solution is grid independent. The verification process was started by running a steady simulation for both Darrieus and Savonius Turbine with a variation in the level of refinement for the mesh. Various levels of mesh have been created by changing the element size inside far field, Hub, Control circuits (CC), blade edge sizing, and number of division for interfaces at a fixed steps for all levels. Four different levels of refinement were tested for the present study and finally, 3rd level of refinement for both Darrieus and Savonius were selected to complete the Analysis.

Coefficient of pressure for the 1st air foil is plotted for the four levels of refinement to determine the mesh convergence limit. 3rd level of refinement having 393901 element number for Darrieus and 313237 element number for Savonius were selected. For this level of refinement, the average values of Orthogonal Quality, aspect ratio, and Skewness for Darrius turbines were found as 0.963, 1.20, and 0.062 respectively. Whereas that of the Savonius turbine were found 0.967, 1.188, 0.059 respectively. These values comes within the acceptable limits that represents a very good quality level [23]. Fig. (8) and (9) shows the variation of pressure coefficient of the air foil and the Semicircular blades respectively.

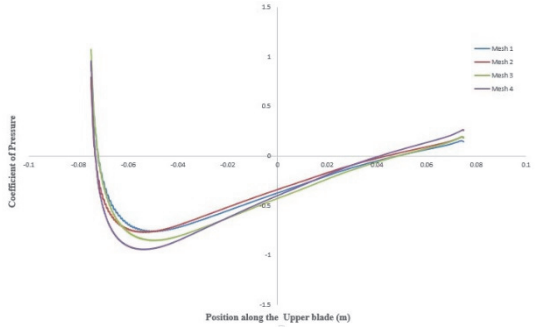

Fig. (8): pressure Coeff .along upper airfoil of Darrius turbine.

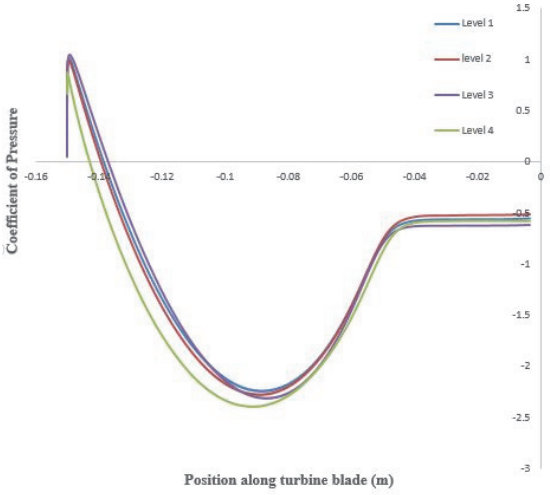

Fig. (9): Pressure Coeff. Along the upper blade of Savonius turbine.

6.6 Simulation Parameters

For Darrieus and Savonius - the Steady and Transient simulations - the water density and viscosity were set to 998.2 kg/m^3 and 1.003 x 10^{-3} kg/m.s respectively. The reference values used in the present analysis is given in table (5) [18]. The

SIMPLE (Semi-Implicit Method for pressure - linked equations) method is used for higher accuracy and to couple the pressure and velocity equations [9] [21] [24]. Gradient is spatial discretization of least square cell-based algorithm is used to insure accurate results. The second order upwind scheme is applied for pressure, momentum, turbulent kinetic energy, and turbulent dissipation rate. Residuals of momentum, continuity, and turbulence equations are set with a convergence criteria of 1 x 10^{-5} [21].

Reference parameter	Value	
	Darrieus	Savonius
Area [m^2]	1	0.3
Density [Kg/m^3]	998.2	
Depth [m]	1	
Enthalpy [j/Kg]	0	
Length [m] ' rotor radius '	0.5	0.15
Pressure [Pa]	0	
Temperature [K]	288.16	
Velocity [m/s]	2 verification and validation 0.5 – 2.5 for analysis	
Ratio of specific heats	1.4	
Reference zone	Hub	

Table 5: Reference values for Both turbines

Transient simulation numerical results depends on the size and number of time steps, however it requires high computational time. Accordingly, in the present study, a 4 degree rotation per time step was applied in order to maintain the accuracy and computational time. In order to reach a steady state, 8 complete revolutions for rotor were simulated [25] and a total of 720 time steps were applied for 50 iteration per each time step.

The coefficient of torque (C_T) was monitored to obtain the mean moment on turbines surface. The C_T of the last revolution was used to calculate the power coefficient. The variation of C_T is studied over the entire range of azimuth positions to evaluate the staring moment and its fluctuations for each turbine.

7. Results and Discussion

7.1 Model Validation

The entire domain was initialized using Standard initialization method. Each turbine was simulated at constant flow speed of 2 m/s over for a range of TSR for the Purpose of validation .Table (6) and (7) give the range of tip speed ratio (TSR), power coefficient (C_P) and time step calculations for Darrieus and Savonius turbines respectively. Simulation ran until both turbines reached a steady state. Coefficient of torque (C_T) was monitored to obtain the mean moment on turbines surface.

Flow Velocity ,v (m/s)	TSR	ω (rad/sec)	Simulation time step, Δt (sec)	Number of revolutions simulated
2	1	4	0.017444444	8
	1.5	6	0.011629630	
	2	8	0.008722222	
	2.5	10	0.006977778	
	3	12	0.005814815	
	3.5	14	0.004984127	

Table 6: Validation tranient calculations for Darriues turbine

Flow Velocity ,v (m/s)	TSR	ω (rad/sec)	Simulation time step, Δt (sec)	Number of revolutions simulated
2	0.4	5.33333	0.013083333	8
	0.6	8	0.008722222	
	0.8	10.6667	0.006541667	
	1	13.3333	0.005233333	

1.2	16	0.004361111

Table 7: Validation transient calculations for Savoniues turbine

For the purpose of results validity, the Validation of Darrieus turbine computational model obtained results was performed for a small 3-bladed H-Darrieus water turbine tested experimentally and 2D simulated by Maitre [24], a 3-bladed H-Darrieus water turbine 2D and 3D simulated by Stefania [26]. The average Error with Maitre 2D model was 5.1% with a Max. Of 7.1% and with Stefania 2D model was 9.2 % with a Max. Of 18%. Fig. (10) Shows a comparison between the numerically predicted and experimentally measured Power Coefficients (C_p) verses tip speed ratio (TSR).

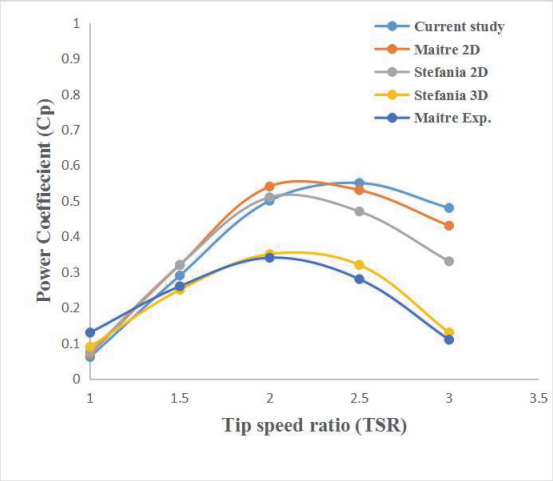

Fig. (10): C_P vs. TSR for Different studies of Darrius turbine.

Savonius turbine Computational model obtained results was performed for a small 2 – bladed semicircular shaped Savonius water turbine tested experimentally and 2D simulated by Parag [27]. Fig. (11) Shows the comparison between the numerically predicted and the experimentally measured power coefficient (C_p) Verses Tip speed ratio (TSR).

It can be noticed that for a Darrieus and Savonius turbine that numerically obtained results overestimated the experimentally obtained results. However, the trend of the Power Coefficient (C_p) over the tip speed ratio (TSR) range is the same for 2D, 3D and experimental data. The reason is that Vortices occurred in the of the Blade ends in 3D simulation and experiment Causes energy losses which is called the 3D effect, where water flows with different velocities (velocity gradient) at the top and bottom of the blades generating a pressure difference pushing water at the end of the blades from high-pressure region to low-pressure region enhancing vortices to be generated [28].

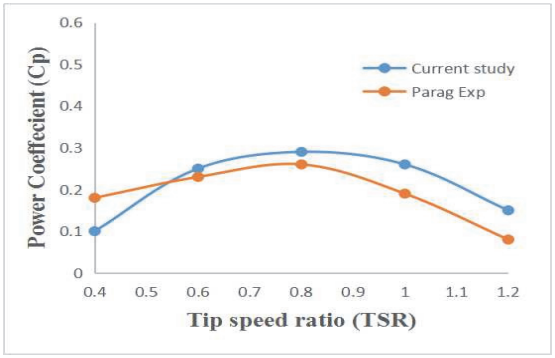

Fig. (11): C_P vs. TSR for Different studies of Savonius turbine.

7.2 Savonius and Darrieus Results

As a result of validation process, the maximum power coefficient (C_p) occurred an optimum tip speed ration of 2.55 as shown Fig (10). Using the obtained optimum tip speed ratio, an analysis for the turbine performance over the range of water speed in the Nile River from 0.5 to 2.5 m/s to was carried to study the variation of the turbine power coefficient (C_p). Fig (12) shows the different values of Power coefficient (C_p) over the desired velocity range. At a flow velocity of 0.5 m/s, C_p has a value 0.5 then it experienced a slight increase over the velocity range till it reaches a maximum of 0.55 at the Nile nominal speed of 2 m/s with a constant behavior a flow velocity of 2.5 m/s.

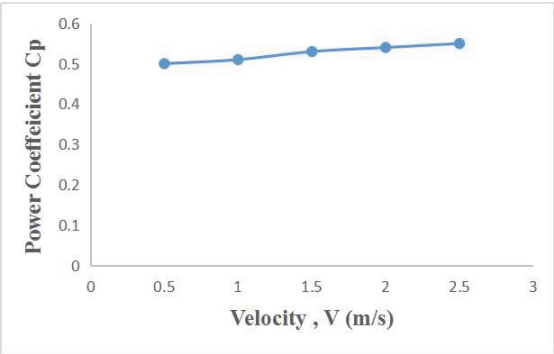

Fig. (12): C_P for a velocity range for a Darrius turbine.

For the Savonius turbine, a maximum power coefficient (C_p) of 0.29 occurred at an optimum tip speed ratio of 0.8 as shown in Fig (11). Using the optimum tip speed ratio, an analysis for the turbine performance over the range of water speed in the Nile River was carried to study the variation of the turbine power coefficient.

Fig (13) gives the different values of power coefficient (C_p) over the desired velocity range. At a flow velocity of 0.5 m/s, C_p has a value of 0.5 then it experienced an increasing behavior reaching a maximum value of 0.29 at a speed of 1.5 m/s then it stayed constant for the rest of the range.

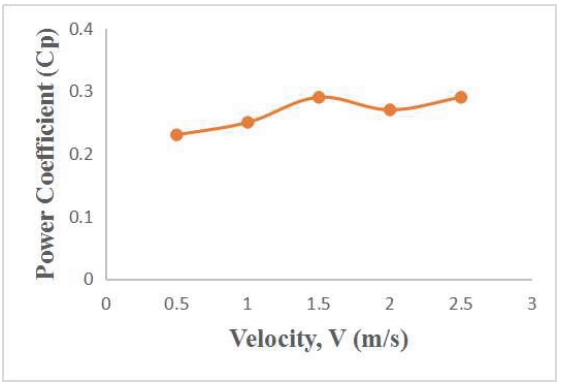

Fig. (13): C_P for a velocity range for a Savonius turbine.

Tables (8) & (9) give the time step calculations and results for Darrius and Savonius turbines analyses respectively.

Flow Velocity ,v (m/s)	TSR	ω (rad/sec)	Simulation time step, Δt (sec)	Number of revolutions simulated
0.5	2.55	2.55	0.027363834	8
1		5.1	0.013681917	
1.5		7.65	0.009121278	
2		10.2	0.006840959	
2.5		12.75	0.005472767	

Table 8: transient analysis calculation for Darrius turbine.

Flow Velocity ,v (m/s)	TSR	ω (rad/sec)	Simulation time step, Δt (sec)	Number of revolutions simulated
0.5	0.8	2.666667	0.026166667	8
1		5.333333	0.013083333	
1.5		8	0.008722222	
2		10.66667	0.006541667	
2.5		13.33333	0.005233333	

Table 9: Transient analysis calculations for Savonius turbine.

Both Turbines were tested in order to investigate the starting torque at the first two revolutions. The coefficient of torque (C_T) is monitored at every time step and the variation of C_T with respect to azimuthal angle is plotted in Fig (14). It can be seen from Fig (14) that the Instantaneous values of C_T at the first two revolutions for Savonius turbine is much higher than Darrieus turbine by two to three times.

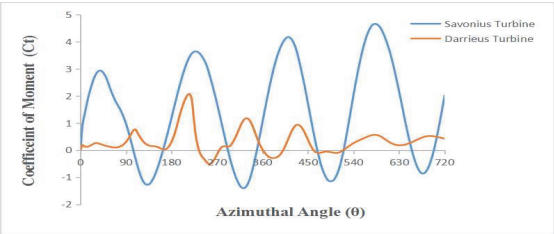

Fig. (14): Starting torque for both Darrius and Savonius Turbines

8. Conclusion

A study of the performance of the 3-bladed Darrieus and 2-bladed semicircular shaped Savonius turbine -with respect to the velocity conditions in the Nile River- was carried out by using 2D simulation analysis of ANSYS CFD module, fluent 19.1. A mesh independence study was carried out to find the optimal mesh quality to assure accurate results. The $k-\varepsilon$ turbulence model was used with a y^+ value equals 1 .Validation for Darrieus and Savonius turbines are made by comparing 2D numerical results obtained with previous validated studies of Maitre [24] & Stefania [26] for Darrieus and Parag [27] for Savonius. For all simulation cases, all initial conditions, boundary conditions and numerical methodology were kept the same.

A maximum power coefficient of 0.55 at a tip speed ratio of 2.55 and flow velocity of 2 m/s for Darrieus turbine and a maximum power coefficient of 0.29 at a tip speed ratio of 0.8 and flow velocity of 1.5 m/s for Savonius turbine was obtained. For the velocity analysis at the optimum tip speed ratio over a range of velocities from 0.5 m/s to 2.5 m/s, power coefficient starts to increase the behaves constantly over the rest of the range for both turbines.

Future work will comprise a 3D Computational and Experimental analysis of present designs of both the Darrius and Savonieus Turbines to obtain even more accurate results of different parameters

Also, an analysis of the performance of a Darrius-Savonius hybrid turbine can be performed using 2D and 3D models to investigate the extent by which the starting torque of the Darrius turbine can be improved while maintaining a high power coefficient (C_P) characteristics.

9. Acknowledgements

We would like to thank his Excellency the president of AASTMT Prof. Ismail Abdelghafar Farag, his Excellency Dean of college of Engineering and technology Prof. Amr Aly & his Excellency the president of marine engineering department in college of Engineering and technology Prof. Ashraf Ibrahim Sharara for facilitating all the procedures required to use the university labs and also we would like to thank everyone who contributed to the completion of this paper.

10. Appendices

Nomenclature

A	*Swept area (m^2)*	Γ_k, Γ_ω	Effective diffusivity for k and ω
c	*Chord (mm)*	$\tilde{G}_k, \tilde{G}_\omega$	Generation of turbulence kinetic energy k and ω
C_T	*Coefficient of torque*	Y_k, Y_ω	Represents the dissipation of k and ω
C_P	*Power Coefficient*	S_k, S_ω	Source term
$\vec{f}$	*Force density [N/m³]*	D_ω	Cross diffusion
k	*Kinetic energy (%)*	ε	Dissipation rate of turbulent kinetic energy
$t, \Delta t$	*Time, time step (s)*	σ_k	constant of standard $k-\varepsilon$ turbulence model

$\vec{u}$	*Velocity (m/s)*	G_k	represents the generation of turbulence kinetic energy due to mean velocity gradients
ρ	*Density (Kg/m³)*		
τ	*Viscous shear stress (Pa)*	G_b	Represents the generation of turbulence kinetic energy due to buoyancy.
θ	*Rotation Angle (rad)*		
λ	*Tip speed ratio*	Y_M	represents the contribution of the fluctuating dilatation incompressible turbulence to overall dissipation rate
ω	*Rotation speed (rad/s)*		
u_j	velocity component	C_2, $C_{1\varepsilon}$	Constants
x_j	*Cartesian coordinate*	α_k, α_ε	the turbulent prandtle numbers for k and ε respecivley
μ	Viscosity	S_k, S_ε	The user defined source terms.
μ_t	Turbulent viscosity	*CFD*	Computational Fluid dynamics

11. References

[1] Güney, M., & Kaygusuz, K. (2010). Hydrokinetic energy conversion systems: A technology status review. Renewable and Sustainable Energy Reviews, 14(9), 2996-3004.

[2] World Economic Outlook. International Monetary Fund, 2015.

[3] Egypt AQUASTAT - FAO's Information System on Water and Agriculture, FAO, 2016.

[4] Akwa JV, Da Silva Alves, Junior G, Petry AP. Discussion on the verification of the overlap ratio influence on performance coefficients of a Savonius wind rotor using computational fluid dynamics. Renew Energy 2012; 38:141–9. https://doi.org/10.1016/j.renene.2011.07.013.

[5] Menet JL. A double-step Savonius rotor for local production of electricity: a design study. Renew Energy 2004; 29:1843–62. https://doi.org/10.1016/j.renene.2004.02.011.

[6] Mohamed MH, Janiga G, Pap E, Thévenin D. Optimal blade shape of a modified

Savonius turbine using an obstacle shielding the returning blade. Energy Convers

Manage 2011; 52:236–42. https://doi.org/10.1016/j.enconman.2010.06.070.

[7] Hau E. Wind turbines: fundamentals, technologies, application, economics.

Berlin: Springer-Verlag; 2006.

[8] Kirke BK. Evaluation of self-starting vertical axis wind turbines for stand-alone

Applications (PhD thesis). Griffith University; 1998.

[9] Mohamed, M. H. (2012). "Performance investigation of H-rotor Darrieus turbine with new airfoil shapes." Energy 47(1): 522-530.

[10] M. Shiono, K. Suzuki, S. Kiho, An experimental study of the characteristics of a
Darrieus turbine for tidal power generation, Electr. Eng. Jpn. 132 (3) (2000)
38e47.

[11] Asr, M. T., et al. (2016). "Study on start-up characteristics of H-Darrieus vertical axis wind turbines comprising NACA 4-digit series blade airfoils." Energy **112**: 528-537.

[12] Mohamed MH, Janiga G, Pap E, Thevenin D. Optimization of Savonius turbines using an obstacle shielding the returning blade. Renew Energy 2010; 35(11): 2618e26.
[13] Alom, N. and U. K. Saha (2019). "Influence of blade profiles on Savonius rotor performance: Numerical simulation and experimental validation." Energy Conversion and Management **186**: 267-277.
[14] Khan NI, Iqbal T, Hinchey M, Masek V. Performance of savonius rotor as a water current turbine. J Ocean Technol 2009; 4(2):71e83.
[15] Kumar, A. and R. P. Saini (2016). "Performance parameters of Savonius type hydrokinetic turbine – A Review." Renewable and Sustainable Energy Reviews **64**: 289-310.
[16] Physik, F. (1984). The Betz optimum efficiency for windmills. Applied Energy, 17, 15–23.
[17] Bianchini A, Balduzzi F, Bachant P, Ferrara G, Ferrari L. Effectiveness of two-dimensional {CFD} simulations for Darrieus VAWTs: a combined numerical and experimental assessment. Energy Convers Manage 2017; 136:318–28. http://dx.doi.org/10.1016/j.enconman.2017.01.026. URL <http://www.sciencedirect.com/science/article/pii/S0196890417300250>.
[18] Joo S, Choi H, et Lee J. Aerodynamic characteristics of two-bladed H-Darrieus at various solidities and rotating speeds. Energy 2015; 90:439–51.
[19] Daróczy L, Janiga G, Petrasch K, et al. Comparative analysis of turbulence models for the aerodynamic simulation of H-Darrieus rotors. Energy 2015; 90:680–90.
[20] Paillard B, Astolfi J, Hauville F. Uranse simulation of an active variable-pitch cross- flow Darrieus tidal turbine: sinusoidal pitch function investigation. Int J Mar Energy
2015; 11:9–26. http://dx.doi.org/10.1016/j.ijome.2015.03.001. URL <http://www.sciencedirect.com/science/article/pii/S2214166915000144>.
[21] Saini, G. and R. P. Saini (2018). "A numerical analysis to study the effect of radius ratio and attachment angle on hybrid hydrokinetic turbine performance." Energy for Sustainable Development **47**: 94-106.
[22] Trivellato, F., & Castelli, M. R. (2014). On the Courant e Friedrichs e Lewy criterion of rotating grids in 2D vertical-axis wind turbine analysis. Renewable Energy, 62, 53–62.
[23] Kumar, A., & Saini, R. P. (2017b). Performance analysis of a single stage modified Savonius hydrokinetic turbine having twisted blades. Renewable Energy, 113, 461–478. https://doi.org/10.1016/j.renene.2017.06.020.
[24] Maître, T., Amet, E., & Pellone, C. (2013). Modeling of the flow in a Darrieus water turbine:
Wall grid refinement analysis and comparison with experiments. Renewable Energy,
51, 497–512
[25] Elbatran, A. H., et al. (2017). "Performance study of ducted nozzle Savonius water turbine, comparison with conventional Savonius turbine." Energy **134**: 566-584.
[26] Zanforlin, S. (2018). "Advantages of vertical axis tidal turbines set in close proximity: A comparative CFD investigation in the English Channel." Ocean Engineering **156**: 358-372.
[27] Talukdar, P. K., et al. (2018). "Parametric analysis of model Savonius hydrokinetic turbines through experimental and computational investigations." Energy Conversion and Management **158**: 36-49.
[28] Zhiyang, Z., et al. (2016). "3-D SIMULATION OF VERTICAL-AXIAL TIDAL CURRENT TURBINE." POLISH MARITIME RESEARCH 23: 73-8